Aeolian slipface dynamics and grainflow morphologies on Earth and Mars

Icarus 314 (2018) 311–326

Contents lists available at ScienceDirect

Icarus

journal homepage: www.elsevier.com/locate/icarus

Aeolian slipface dynamics and grainflow morphologies on Earth and Mars

Carin Cornwall[a,*], Mary C. Bourke[b], Derek W.T. Jackson[a], J.Andrew G. Cooper[a,c]

[a] School of Environmental Science, Ulster University, Coleraine, United Kingdom
[b] Department of Geography, Trinity College, Dublin, Ireland
[c] Geological Sciences, School of Agricultural, Earth and Environmental Sciences, University of KwaZulu-Natal, South Africa

A B S T R A C T

In 2015, an active dune field on Mars was visited up close by the Curiosity rover in Gale Crater providing the first high resolution ground images of fine scale windblown features not previously resolved from orbital-based imagery. For the first time, these images allow for direct comparison with terrestrial aeolian dynamics and provide critical ground truth data to bridge the gap between model predictions and satellite observations. The image data from the slipface on the Namib dune within the Bagnold dune field shows grainflow morphologies that are similar to dunes on Earth. Quantitative estimates of flow thickness, based on shadow length are presented for the grainflows on the Namib dune slipface and compared to grainflow characteristics measured by terrestrial laser scans from the Maspalomas dune field located in Gran Canaria, Spain. Using observations from Maspalomas to support interpretations of martian slipface dynamics, we discuss implications for the local wind regime, style of grainflow, seasonal activity, and dune migration. The presence of multiple large-magnitude grainflows on the Namib slipface suggests an active aeolian environment, capable of delivering enough sediment to the slipface to initiate these flows and transport sediment to the bottom of the lee slope. However, the thinness of grainflows on the Namib dune, the formation of smaller grainflows directly below the dune brink and limited grainfall suggest a lower wind energy environment, at least for the most recent slipface activity. Large, actively migrating stoss ripples obliquely oriented to the dune crest regularly deposit sediment on to the upper slipface and may be a mechanism in which larger grainflow occur during seemingly low energy wind events. This mechanism of sediment delivery may also explain the existence of a variety of slipface morphologies, both young and old, which are otherwise quickly erased on Earth due to sediment redistribution and grainfall.

1. Introduction

The surface of Mars is dominated by aeolian processes which have operated effectively over billions of years. In the absence of in situ observation, studies on martian dune dynamics have relied on atmospheric modelling (e.g. Anderson et al., 1999; Fenton et al., 2005; Hayward et al., 2009; Jackson et al., 2015) and high-resolution satellite images to analyze morphology, and record change (e.g. Fenton et al., 2005; Fenton, 2006; Bridges et al., 2007; Hayward et al., 2007; Bourke et al., 2008; Hayward et al., 2009; Hobbs et al., 2010; Silvestro et al., 2010; Bridges et al., 2011; Silvestro et al., 2011; Bridges et al., 2013; Silvestro et al., 2013; Cardinale et al., 2012; Cardinale et al., 2016). Through the careful analysis of annual ripple migration and multiple years of repeat High Resolution Imaging Science Experiment (HiRISE) images from the Mars Reconnaissance Orbiter, estimates of dune migration rates have been determined for various dune fields on Mars and range from 0.1 to 12 m/Mars year (Bridges et al., 2007; Bourke et al., 2008; Silvestro et al., 2010; Bridges et al., 2011; Chojnacki et al., 2011; Hansen et al., 2011; Silvestro et al., 2011; Bridges et al., 2012a,b; Bridges et al., 2013; Geissler et al., 2013; Silvestro et al., 2013; Chojnacki et al., 2015; Cardinale et al., 2016; Runyon et al., 2017). Mars dunes generally migrate at a slower rate than most terrestrial dunes of similar morphology (e.g. Finkel, 1959; Long and Sharp, 1964; Hastenrath, 1967; Pye and Tsoar, 1990; Jimenez et al., 1999; Dong et al., 2000; Vermeesch and Drake, 2008) but are comparable to some small dome and barchan dunes having migration rates between 4 and 8 m/Earth year (Dong et al., 2000; Bristow and Lancaster, 2004) as well as dunes found in Antarctica, having migration rates of about 1.5 m/Earth year (Bourke et al., 2009b).

Dune migration is largely accomplished through a series of individual grainflows that transport sediment from the stoss slope to the bottom of the lee slope, advancing the slipface. In addition, grainflow formation patterns, morphology, and frequency reflect characteristics of the environment in which they occur such as wind velocity, sediment properties, and climate (e.g. Allen, 1968; Allen, 1970; McKee and Bigarella, 1972; Morris et al., 1972; Sweet and Kocurek, 1990;

* Corresponding author.
E-mail address: cornwall-c@email.ulster.ac.uk (C. Cornwall).

https://doi.org/10.1016/j.icarus.2018.05.033
Received 27 October 2017; Received in revised form 29 April 2018; Accepted 29 May 2018
Available online 02 June 2018

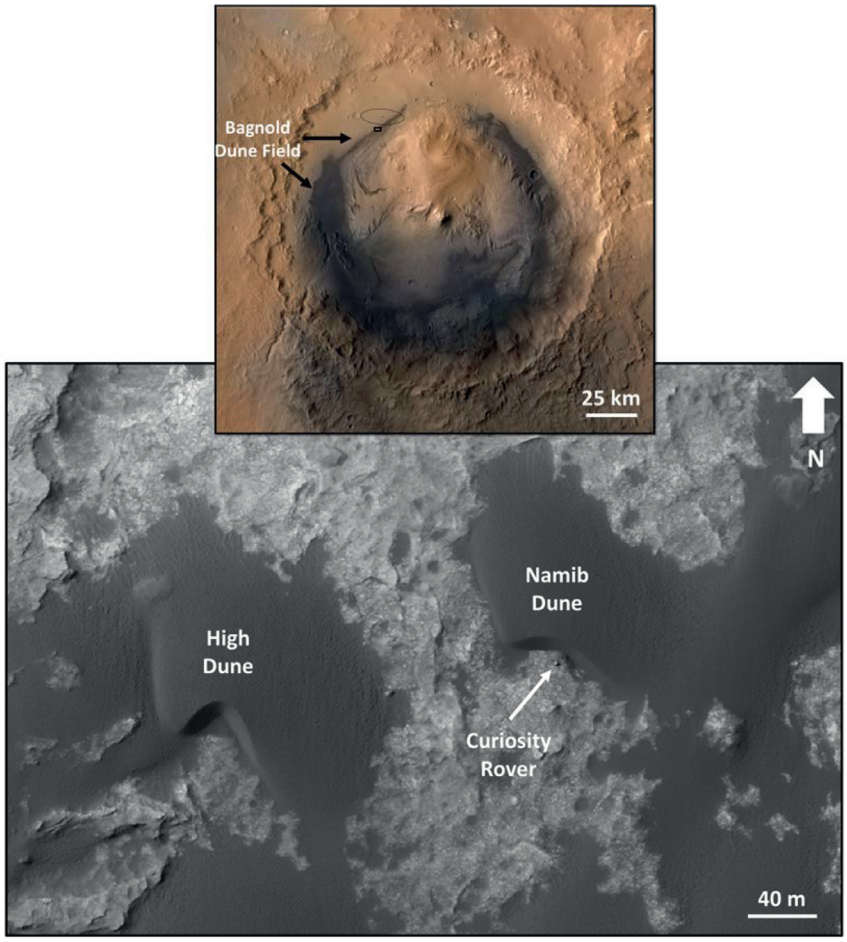

Fig. 1. Top: CTX/HRSC/Viking composite mosaic showing the location of the Namib dune on Mars (black rectangle below the Curiosity landing site oval) in relation to the Bagnold dune field. Bottom: HiRISE image ESP_044172_1755 of the Namib dune and neighboring High dune with the curiosity rover in front of the Namib dune slipface. Dashed lines on the Namib dune are the approximate extents of the western central, and eastern portions of the slipface shown in Figs. 2–4, respectively.

McDonald and Anderson, 1992; McDonald and Anderson, 1995; McDonald and Anderson, 1996; Nickling et al., 2002; Cupp et al., 2005; Breton et al., 2008; Sutton, 2012; Sutton et al., 2013a,b; Pelletier et al., 2015; Nield et al., 2017; Cornwall et al., 2018). Therefore, the study of grainflows is an integral part of dune dynamics and climate interpretation. Excluding the largest of grainflows, it is nearly impossible to discern details of slipface activity on Mars from HiRISE satellite images which have a resolution of 25 cm/pixel. The Curiosity rover provided the first high resolution ground images of an active dune slipface on the Namib dune in the Bagnold dune field in Gale Crater (Fig. 1) opening a unique opportunity for a more detailed study of aeolian features on Mars. For the first time, these images allow for a direct comparison between terrestrial slipface processes and those currently in operation on Mars.

1.1. Grainflow formation

Terrestrial studies have reported mechanisms for slipface grainflow initiation that include localized over-steepening, slump degeneration, destabilization from larger grainflows or disturbance of a mid-slope 'lock up zone', and complex airflow patterns. Localized over-steepening of the lee slope typically occurs tens of centimeters below the dune brink where saltating grains of sediment are deposited from the stoss slope (e.g. Allen, 1968; Allen, 1970; Borowka, 1979; Hunter, 1985; Anderson, 1988; McDonald and Anderson, 1992; McDonald and Anderson, 1995; Nickling et al., 2002; Walker and Nickling, 2002; Cupp et al., 2005; Kok et al., 2012; Sutton, 2012; Sutton et al., 2013a,b). When the deposited sediment exceeds the critical angle of repose of the grains, failure occurs, forming an alcove that spreads laterally upslope toward the dune brink and a depositional lobe of sediment that spreads laterally downslope and accumulates below the alcove (e.g. Allen, 1968; Allen, 1970; Hunter, 1977; Borowka, 1979; Fryberger and Schenk, 1981; Hunter, 1985; Anderson, 1988; McDonald and Anderson, 1992; McDonald and Anderson, 1995; Tischer et al., 2001; Nickling et al., 2002; Walker and Nickling, 2002; Cupp et al., 2005; Dasgupta and Manna, 2011; Kok et al., 2012; Sutton, 2012; Sutton et al., 2013a,b; Cornwall et al., 2018; Nield et al., 2017).

Slump degeneration was first described by Fryberger and Schenk (1981) as an alternative to the grainflows that formed alcoves. During wind tunnel experiments, these alternative grainflows were observed to initiate as a series of tensional features near the top of the slipface. As the flow progressed, compressional features (folds) formed in places where the sediment slowed and overrode parts of the flow, resulting in a 'slump sheet' of sediment with minor deformational structures in cross-section, suggesting a form of dry cohesion (Fryberger and Schenk, 1981). Slump degeneration has not been studied in depth but may also have been observed by HYPERLINK \l "bib104" Sutton et al. (2013b) as small non-cohesive slabs or larger features (meters across), termed slab flows as well as in the coastal dunes of the Maspalomas dune field (Cornwall et al., 2018). It is unknown what caused the dry cohesion observed by Fryberger and Schenk (1981) but during field observation, it is probable that cohesion of dune sediment may arise with the presence of moisture (liquid or ice) in the subsurface sediment layers or due to induration from soluble

salts.

Smaller grainflows may initiate due to disturbances from larger grainflow activity (Breton et al., 2008; Cornwall et al., 2018) or from the destabilization of the mid slipface slope in a region where suspended sediment settles, creating a secondary location of localized over-steepening (McDonald and Anderson, 1992, 1995, 1996; Nickling et al., 2002; Nield et al., 2017). The accumulation and over-steepening of sediment mid slope may also be enhanced by grainflows that did not successfully deliver sediment to the base of the slipface. Sediment transport from these flows is halted in a 'lock up zone', partway down the slipface where sediment from other smaller grainflows also accumulates (McDonald and Anderson, 1992, 1995, 1996).

The role of airflow on the lee side of a dune may also influence grainflow activity, where secondary air flow patterns generated by flow separation at the dune crest and the subsequent reattachment flow may produce complex eddies and vortices (Parsons et al., 2004a,b; Jackson et al., 2013a,b; Smith et al., 2017). Though not well understood, these secondary flow patterns may have a significant impact on surface shear stress, resulting in sediment redistribution on the slipface (e.g. Wiggs, 2001; Nickling et al., 2002; Walker and Nickling, 2002; Cupp et al., 2005). For example, incident airflow oriented between 25° to 90° to the slipface on a dune may produce deflected flow on the slipface in the form of 2D eddies and 3D vortices (Sweet and Kocurek, 1990; Eastwood et al., 2012) resulting in lateral transport of sediment (Walker, 1999). In addition, greater wind velocities have been shown to decrease the angle of initial yield, resulting in grainflow activity at lower critical angles than otherwise possible (Pelletier et al., 2015).

1.2. Comparing terrestrial grainflow activity to Mars

Terrestrial dunes are highly dynamic and under wind conditions conducive to grainflow activity, relict structures such as ripples and older grainflows are quickly erased by grainfall or redistribution of sediment (e.g. Bagnold, 1941; Allen, 1970; Hunter, 1977; Hunter, 1985; Anderson, 1988; McDonald and Anderson, 1995; Kok et al., 2012; Cornwall et al., 2018). Martian aeolian dynamics operate under significantly thinner atmospheric conditions compared to Earth (< ~1.7% of Earth's surface atmospheric density) and lower surface gravity about 38% of Earth's gravity (Bridges et al., 2017). The fluid threshold of grain saltation therefore requires much greater wind speeds compared to Earth. Lander measurements and atmospheric circulation models have indicated that these above-threshold speeds are rare, contradicting observations of sand-sized particles moving across the planet surface (Zurek et al., 1992; Sullivan et al., 2000; Haberle et al., 2003; Fenton et al., 2005). However, sand saltation may be possible at lower wind speeds through the development of saltation clusters via self-sustaining saltation trajectories from grains that are sporadically mobilized due to a passing eddy (Sullivan & Kok, 2017). Once a grain is in motion, it is easier to maintain saltation on the martian surface. Due to the lower gravity and vertical drag, saltating grains have higher and longer trajectories (Almeida et al., 2008; Kok, 2010a,b; Kok et al., 2012). Grains are airborne for a longer period of time resulting in a prolonged acceleration by wind which produces an impact threshold comparable to terrestrial values, thus capable of setting other grains in motion upon collision (Greeley and Iversen, 1985; Greeley, 2002; Nickling, 1988; Merrison et al., 2007; Claudin and Andreotti, 2006; Almeida et al., 2008; Kok, 2010a,b).

A variety of aeolian structures related to grain saltation are visible on the Namib dune on Mars. The stoss slope features two scales of ripples, where the smaller bedforms, identified as impact ripples, are superimposed on top of large ripples with an average wavelength of about two meters (Lapotre et al., 2016). The large ripples form a ladder back pattern, where the ripple crestlines are oriented NW and NE (Silvestro et al., 2013; Lapotre et al., 2016) and intersect the barchan dune brink obliquely along the horns and transverse in the center (Ewing et al., 2017). There are two slipface surfaces present on the Namib dune, where the primary slipface faces toward the south and the secondary slipface is located along the western flank of the dune (Ewing et al., 2017). The primary slipface of the Namib dune is complex, having a mixture of a series of overlapping older and younger grainflows with indications of slumping, little evidence of widespread grainfall, and ongoing impact ripple formation (Ewing et al., 2017). In general, grainflow processes dominate the central portion of the primary slipface while impact ripple formation, parallel to the slipface, and grainfall deposits dominate the horn slipface slopes (Ewing et al., 2017). The secondary slipface is dominated by large ripples that migrate obliquely downslope toward the south and intersects with the western horn of the dune (Ewing et al., 2017).

Mars experiences seasonal cycles of aeolian activity and inactivity, where the southern winter solstice is a quiet period with limited ripple movement and infrequent grainflows (e.g. Ayoub et al., 2014; Hansen et al., 2011; Bridges et al., 2017). During this time, grain movement is most likely driven by periodic gusts of wind and any activity that occurs is sporadic (Bridges et al., 2017). In the absence of dynamic observations and an opportunity to revisit the Namib dune throughout the martian year, the flow morphology and location of these grainflow events may have preserved information about the latest grainflow event and the aeolian conditions that produced them.

We investigate the differences and similarities of terrestrial and martian slipface dynamics using a dune in the Maspalomas dune field in Gran Canaria, Spain as an analog to the grainflow activity preserved on the Namib dune slipface in Gale crater, Mars (Figs. 2–5). This study applies the classification scheme of grainflow morphologies proposed by Cornwall et al. (2018; Fig. 6) to Mars grainflows and an interpretation of the local wind regime responsible for the most recent grainflow activity, is presented, supported by terrestrial field observations of grainflow morphodynamics. Estimates of the grainflow thickness of the freshest flows on the Namib slipface and volumes calculations are provided for each grainflow and compared to grainflow thicknesses and volumes measured in the Maspalomas dune field, Gran Canaria, Spain. Estimates of flow volume provide an indication of the effectiveness of slipface processes on the Namib dune for the most recent grainflow activity and may also provide some insights into dune migration patterns in the Bagnold dune field. Lastly, we discuss the factors that influence grainflow initiation and their formation patterns as well as implications for seasonal slipface activity and dune migration.

Grainflows on Earth have been the key to understanding aeolianites and paleoenvironments (McKee et al., 1971; McKee and Bigarella, 1972; Morris et al., 1972; Bigarella, 1975; Hunter, 1977; Bourke, 2005; Grotzinger et al., 2005; Eastwood et al., 2012). In a similar fashion, the aeolian record on Mars potentially contains valuable insights into the geologic history of the planet, aiding in the interpretation of martian aeolianites such as those found at Meridiani Planum (Grotzinger et al., 2005) or the cross-bedded sandstone of the Stimson formation; part of the basal flank of Aeolis Mons (aka Mount Sharp) in Gale Crater, Mars (HYPERLINK \l "bib8" Banham et al., 2018).

2. Methodology

2.1. Earth and Mars study sites

The Maspalomas study site (27.744° N, −15.573° W), used as an analog to the martian Namib dune slipface features (−4.686° N, 222.364° W) in this study, is described in detail in Cornwall et al. (2018) and Jackson et al. (2013b). The Maspalomas dune field was chosen for an analog because the dry climate, having < 100 mm/year precipitation (Marzol, 1987), with sparse vegetation growth, and regular slipface activity, made it a convenient location to study the morphometrics of typical arid dune grainflows. We apply the classification of grainflow morphologies from Cornwall et al. (2018) including hourglass, slab, lobe and funnel flows

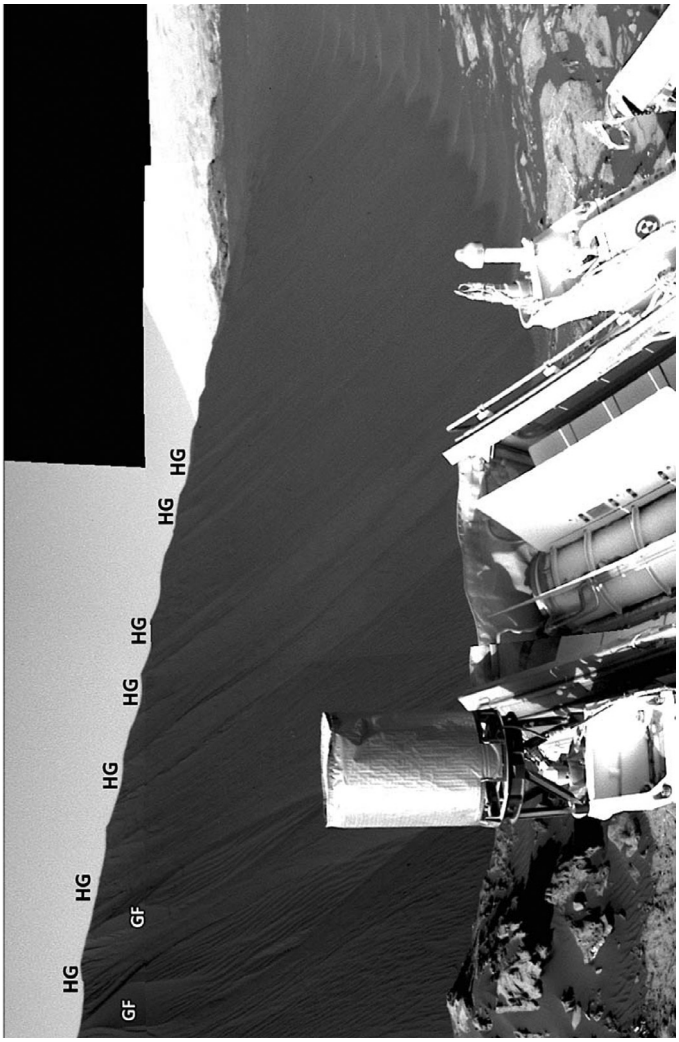

Fig. 2. Right-hand side (eastern horn) of the Namib dune lee slope showing multiple grainflows, ripples, and some grainfall deposits with the Curiosity rover in the foreground. Image is mosaic of 23 images taken by the mast-mounted Left Navigation Camera (Navcam) on December 18, 2015 (mission Sol 1196), providing a 360-degree cylindrical-perspective projection panorama centered at 125° azimuth. Local mean solar time for image exposures was 4 PM. 'GF' signifies grainfall and 'HG' signifies hourglass grainflow.

to the grainflow activity on the Namib dune (Fig. 5a) imaged by the Mars Curiosity rover. The Maspalomas slipface observations were collected on a portion of a transverse dune, having a height of 2.2 m with a slipface angle of 32.15° (Cornwall et al., 2018). The Namib dune is a barchan dune having a height of about 4 m and an average slipface slope of 29° with the slope exceeding 35° in a few locations (Ewing et al., 2017).

Grain sizes collected in the Maspalomas dune field study site ranged from 136 to 522 μm, averaging 244 μm (Cornwall et al., 2018), and were composed of biogenic marine materials (Hernandez et al., 2002) and phonolitic rocks (Martinez, 1986). Sediments from the Namib dune are mafic with the most abundant crystalline phases being plagioclase, olivine and pyroxenes as well as a large component of amorphous material (Bridges et al., 2016; Achilles et al., 2017; Cousin et al., 2017; Ehlmann et al., 2017; Johnson et al., 2017; Lapotre et al., 2017; O' Connell-Cooper et al., 2017). The median grain size of the Namib dune sediments was much finer than the sand grains in Maspalomas and ranged from 100 to 150 μm, or very fine sand (Ewing et al., 2017; Sullivan and Kok, 2017) with a few isolated coarser grains (Ehlmann et al., 2017).

2.2. Wind regime

Fig. 7 shows a comparison of an Earth year of available wind data (from February through September) collected near the Maspalomas study site (Cornwall et al., 2018) and wind data from the Curiosity rover in Gale Crater, Mars. Wind data for the Maspalomas dune field was collected by the Playa del Ingles meteorology station approximately 450 m southeast from the study site at a height of 3 m. Gale Crater wind data, collected by the Rover Environmental Monitoring Station (REMS; Gomez-Elvira et al., 2012) Mars Science Laboratory (MSL) Curiosity mission at a height of 1.5 m was retrieved from the Planetary Data System (PDS) website. Wind data was taken from sols 884 to 1485 of the Curiosity Mission to overlap with observations at the Namib dune. An entire Mars year of wind data centered on the Curiosity rover's visit to the Namib dune was originally planned to be included but some measurements were unreliable or nonexistent and no data was collected after sol 1485. As a result, there are about 86 sols out of one martian year (687 sols) that are not displayed.

The REMS data is treated with caution as the loss of one of the two wind sensors on the rover made reliable determination of wind speed and direction difficult (Pla-Garcia et al., 2016). In addition, wind data was collected throughout Curiosity's traverse and daily variations may reflect influences from local topography especially as the rover

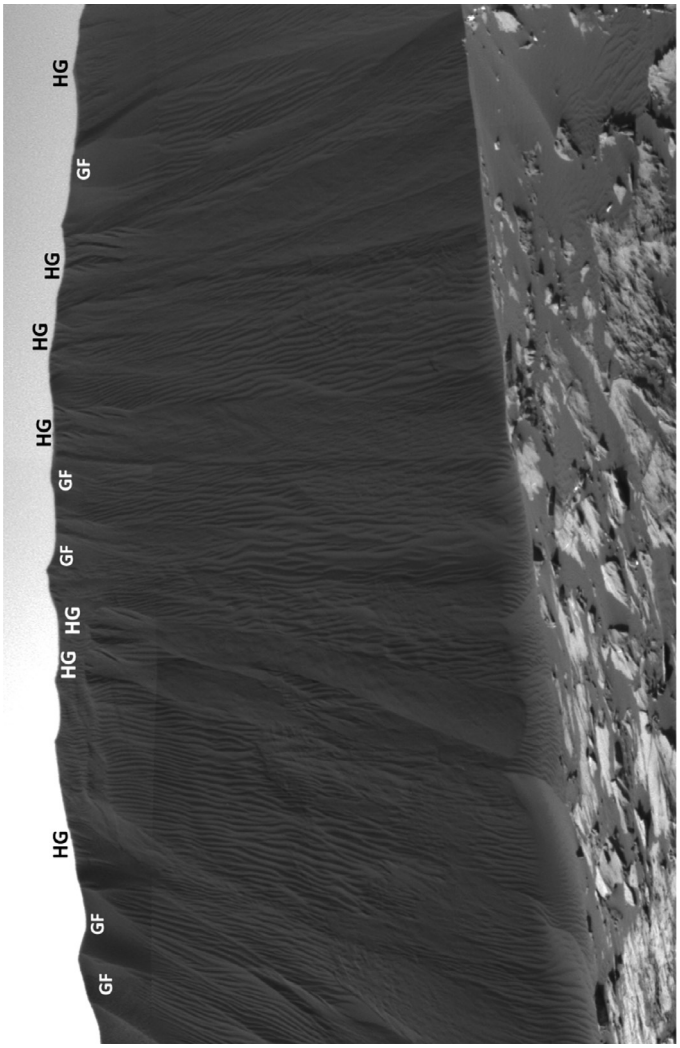

Fig. 3. Same as Fig. 2 but for the central portion of the Namib dune slipface. This section of the slipface contains the freshest grainflows, well-defined ripples and very little evidence of grainfall.

approached Mount Sharp. To ensure more reliable wind sampling was used in this study, Mars wind data was restricted by the wind sensor confidence level for every sol. Observations with weakened data reliability due to temperatures $< -50\,^{\circ}C$, electronic noise, rover movement, incorrect wind sensor configuration, and rear wind direction were excluded. Despite the uncertainties introduced by sensor limitations and changing topography, we are confident in using REMS wind data to compare the wind regime of the Maspalomas study site to Gale crater because the derived wind directions from REMS have shown good agreement with the Mars Regional Atmospheric Modeling System (MRAMS; Pla-Garcia et al., 2016) and the Mars Weather Research and Forecasting (WRF) numerical model (Newman et al., 2017). However, there remain discrepancies between wind velocity measurements from the rover and model predictions but these differences may, in part, be due to complex airflow patterns from local topography not resolved by the models (Pla-Garcia et al., 2016; Newman et al., 2017). Velocity measurements from the rover are valuable in this study because the complex airflow patterns that affect wind speed are unresolved by mesoscale models. These near surface wind speeds are responsible for sediment transport at the dune scale and constrain periods of grainflow activity on the Namib dune.

2.3. Mars grainflow thickness

Measurements of Maspalomas grainflow characteristics were collected using a high-resolution ground-based terrestrial laser scanner (TLS; Cornwall et al., 2018). Spatial estimates of grainflow width, length and area of a couple flows on the primary Namib slipface were previously made by Ewing et al. (2017). This study builds upon these measurements by estimating grainflow thickness and calculating the volume of redistributed sediment for the freshest grainflows on a portion of the Namib slipface. In the absence of data (i.e. Mastcam DEMs) that can resolve grainflow thickness on the Namib dune, flow thickness and subsequent volume estimates for the Namib slipface were trigonometrically estimated using shadow length and the sun's elevation (Table 1; Curran, 1985). If the sun geometry is known, shadow lengths can be utilized to estimate the heights of the objects that cast them in two dimensional images. This a common spatial analysis technique practiced in remote sensing, specifically with high resolution satellite images (e.g. Huertas and Nevatia, 1988; Liow and Pavlidis, 1990; Shettigara and Sumerling, 1998). In a similar fashion, this technique is used for the shadows cast by grainflows on the slipface of the Namib dune, using Mastcam images 1200ML0054960060503183C00_DXXX and 1200ML0054960130503190C00_DXXX. The sun's elevation for each image was approximately 51.63° and 51.93 at the time the images were acquired at 12:18 and 12:20 LMST, respectively. Grainflow thickness was thus calculated by:

$$T = (\text{ShadowLength})*\tan(\text{SunElevation})$$

Only the freshest of grainflows cast a significant enough shadow to be

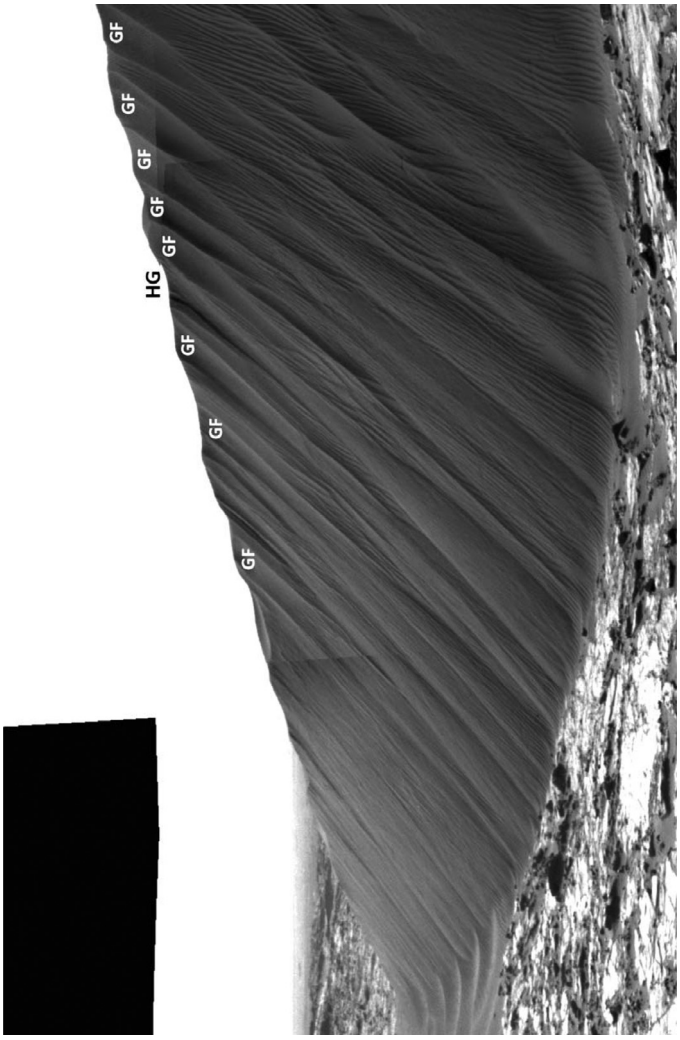

Fig. 4. Same as Fig. 2 but for the left-hand side (western horn) or the Namib dune slipface. Multiple grainflows can be seen and there is evidence of grainfall along the upper lee slope.

measured and so thickness measurements were limited to the most recent grainflow activity.

Since the Mastcam images were not orthorectified in this study, foreshortening of the Mastcam image mosaic was accounted for using a spatial analysis technique involving perspective distortion to derive reliable estimates of grainflow shadows at particular locations on the dune. Perspective distortion occurs when there is a relative scale of nearby and distant features in a two-dimensional image, such as the base of the Namib dune and the brink. Perspective distortion is linear and dependent on distance. Therefore, knowing the distance of the Curiosity rover from the dune (~15 m) and the approximate height of the Namib dune, a focal length can be determined at any point on the dune slipface (e.g. brink or mid slope) with an adjusted pixel scale for the features being measured (Fig. 8).

To assess the accuracy of our pixel-scale correction based on focal length, we compared our estimates with measurements from the Mastcam DEM of Ewing et al. (2017). Using our technique, the two grainflows from Fig. 5 were measured. We estimated a scarp width of 58 cm (vs. 54 cm from the DEM) and a lobe width of 60 cm (vs. 57 cm from the DEM) for the smaller grainflow, and a scarp width of 64 cm (vs. 67 cm from the DEM) and a lobe width of 65 cm (vs. 66 cm from the DEM) for the larger grainflow. The two measurements appear to be in good agreement and measurements of grainflow shadows are considered reliable estimates. Measurement estimates of grainflow length were not attempted for the larger grainflows using an adjusted resolution based on perspective because the vertical resolution changes dramatically down the slope of the slipface. Measurements of area for smaller grainflows near the dune brink were collected, where changes in vertical resolution were minimal. In addition, measurements were restricted to the central portion of the slipface where measurements were the most reliable and image distortion from perspective angles and curvature of the dune limbs were minimal.

The reliability of the grainflow thickness estimates for Mars were additionally tested by conducting a similar calculation for the observations from Maspalomas and comparing the derived measurements to TLS data. The trigonometrically-derived thicknesses for base grainflow thickness in Maspalomas were within ± 0.30 cm of the values recorded by TLS which accurately recorded grainflow attributes on the submillimeter-scale (Cornwall et al., 2018). Grainflow areas of the smaller grainflows in Table 1 and Fig. 5 were calculated using ArcMap and sediment volume estimates for each grainflow were determined using the volume of a wedge to approximate the thickening of a grainflow downslope, following the convention of Cornwall et al. (2018).

3. Results

The Maspalomas dune slipface in Gran Canaria, Spain and the Namib dune slipface on Mars have many similarities in regards to grainflow morphology. Both slipfaces displayed hourglass grainflows as

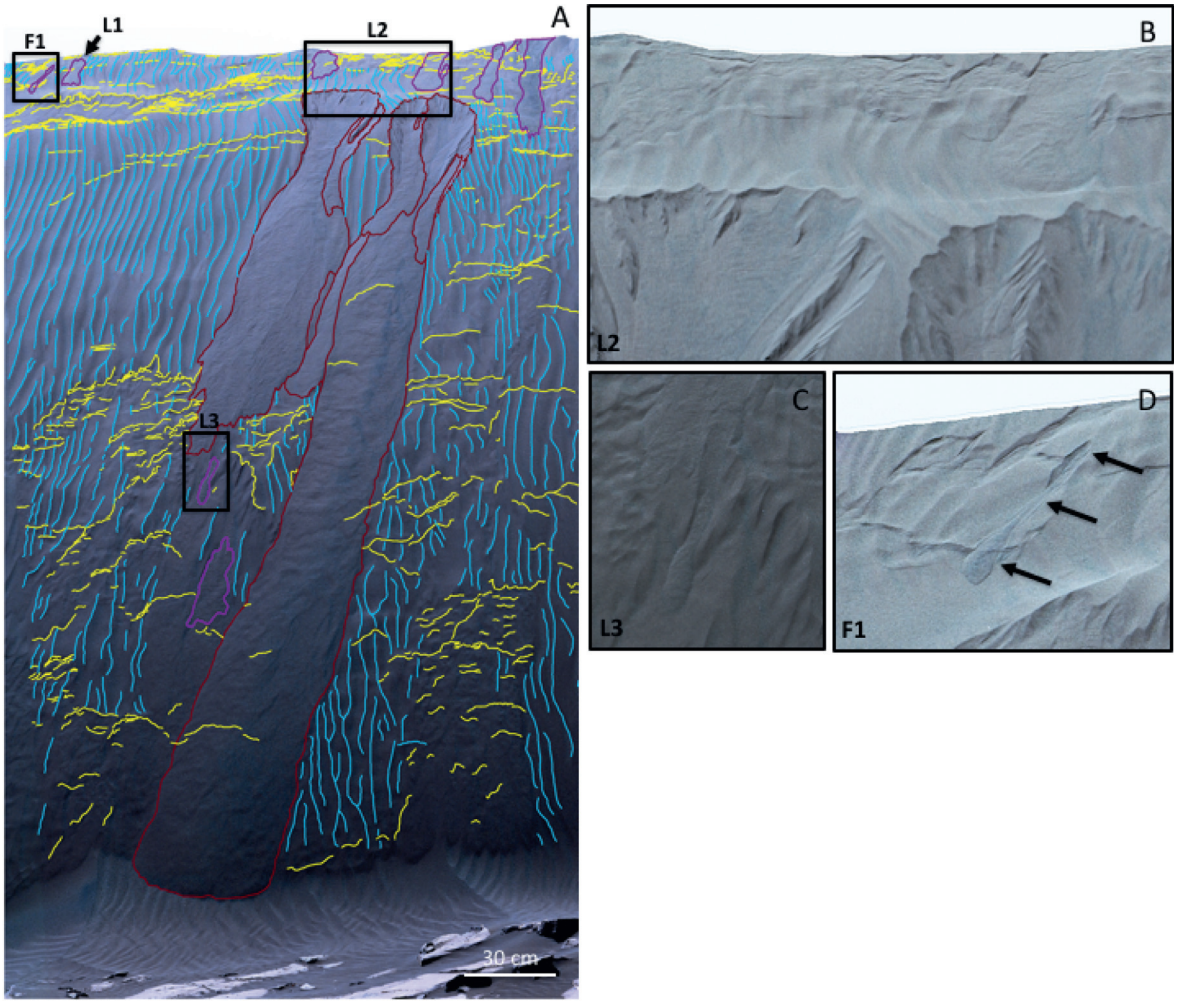

Fig. 5. Map of the grainflow morphology and slipface activity on the Namib dune of the Curiosity mission on Mars (A). Mapped morphologies include: tensional cracks (yellow), ripples (blue), hourglass-shaped grainflows (red), and secondary grainflows (magenta), where lobes are labeled with 'L' and funnels 'F' and correlate to the labels in Table 1. The two hourglass flows shown in (A) correlate with flows H1 and H2 in Fig. 4. Panels B-D show magnifications of some of the secondary flows identified on the slipface. Panels B and C show details of lobe flows and panel D shows a funnel flow. Mapping was done in ArcMap 10.3.1. using Mastcam R0 mosaic image MCAM05491 which was taken on sol 1198 using the Curiosity's Mast Camera telephoto-lens camera. (For interpretation of the references to colour in this figure legend, the reader is referred to the web version of this article.).

well as smaller lobe and funnel flows. However, there were minor morphometric differences.

3.1. Hourglass grainflows

Measurements were performed on the two freshest hourglass grainflows on the Namib dune (Figs. 3 and 5). These grainflows were larger than the Maspalomas hourglass grainflows in area but thinner in flow thickness (Table 1). The estimated Namib hourglass grainflow areas were approximately 16,500 cm^2 and 39,600 cm^2 and the average area for Maspalomas grainflows was approximately 11,000 cm^2 (Table 1; Fig. 9). The deposit thickness at the base of the grainflow for both Namib hourglass flows was below the average for those observed in Maspalomas by more than 1 cm (Table 1; Cornwall et al., 2018). The larger Namib dune hourglass flow had a volume estimate of approximately 7300 cm^3, significantly below the terrestrial average observed in Maspalomas (~22,000 cm^3), despite having a larger planform area (Fig. 9).

3.2. Lobe and funnel grainflows

Lobe and funnel grainflows were a frequent occurrence on the Maspalomas dune slipface, forming on average every minute, and tended to initiate mid-slope (Cornwall et al., 2018). Based on these field observations, the occurrence of small grainflows on the primary Namib slipface was significantly less than expected, where only a few lobe and funnel flows could be identified on the central portion of the slipface (Fig. 5). In contrast to Maspalomas observations, lobe and funnel grainflow activity on the Namib dune favored initiation near the dune brink (Fig. 5a, b and d), almost completely independent from disturbances from hourglass flows apart from one small lobe flow (Fig. 5c). Funnel grainflows were extremely rare. Only one was identified on the portion of the Namib slipface that was mapped (Fig. 5a and d). In contrast to some of the lobe and funnel grainflows observed on the Maspalomas slipface, none of the smaller Namib grainflows identified in this study successfully transported sediment to the base of the slipface. Outside the primary slipface, a number of smaller grainflows were identified on the lee slopes of large ripples migrating obliquely to the secondary slipface along the western flank of the Namib dune (Lapotre et al., 2016; Ewing et al., 2017).

Of the freshest lobe and funnel flows on the Namib, grainflow area ranged between 51 and 580 cm^2, smaller than the typical Maspalomas lobe and funnel flows (Table 1, Fig. 9). In addition, the small grainflows on the Namib dune primary slipface were also significantly thinner than

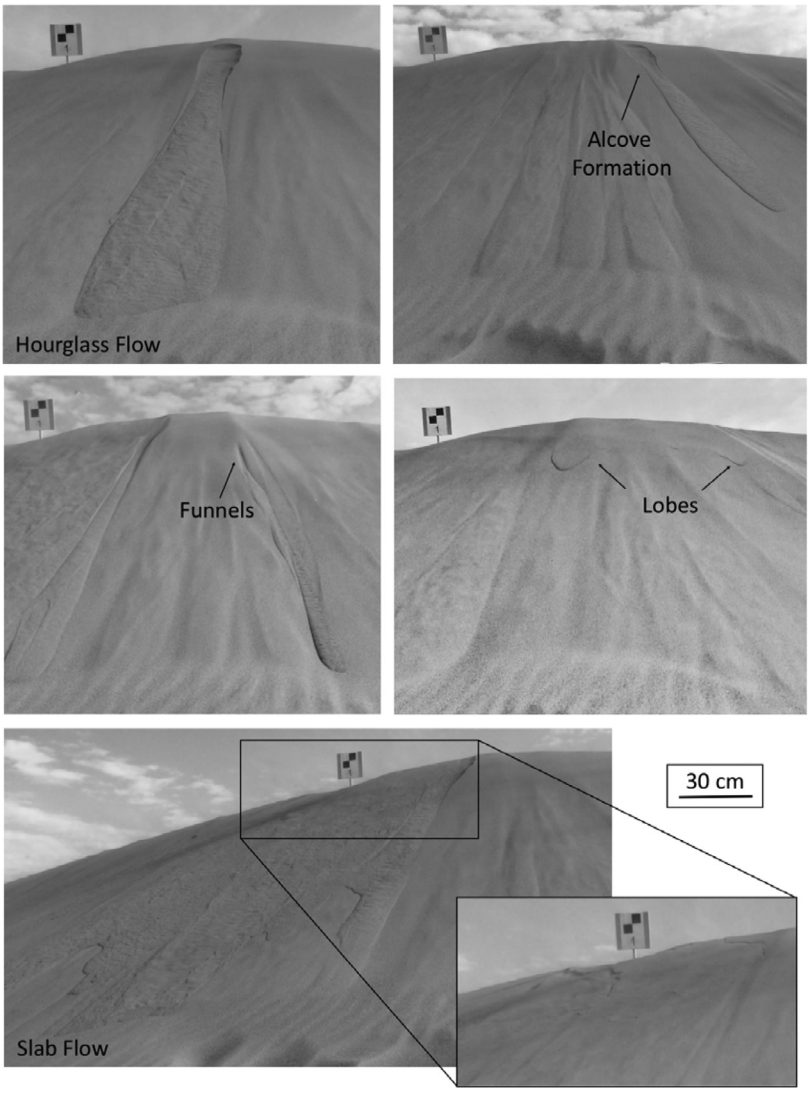

Fig. 6. Grainflow morphologies identified in the Maspalomas dune field, Gran Canaria, Spain, including hourglass grainflows accompanied by the formation of an alcove, smaller funnel and lobe flows, and slab flows that affect large areas of an entire slipface. The checkered A4 paper (21 × 29.7 cm) on target board at the crest of the dune was used for GPS registration and can be used for background scale of the slipface. A foreground scale is provided. Slipface height is approximately 2.2 m.

their terrestrial counterparts, where Maspalomas lobe and funnel flows averaged about a 1 cm thickness while the Namib flows averaged approximately 0.37 cm (Table 1; Fig. 9).

3.3. Tensional cracks

Multiple tensional cracks were identified on the surface of the Namib slipface (yellow lines; Fig. 5a). Similar generally horizontal tensional cracks were observed on the Maspalomas slipface but these features always preceded a slab flow (Cornwall et al., 2018; Fig. 10). Slab flows initiated centimeters below the dune brink and affected large areas (typically meters across) of the slipface and moved large volumes of sediment (Table 1; Fig. 9) compared to hourglass and lobe or funnel grainflows. The tensional cracks on the Namib slipface are pervasive in a region where there appears to be a slump feature or separation of sediment from the dune brink (Figs. 3 and 5a and b). On a much smaller scale, tensional cracks and slump features also appeared to be present on the downwind slopes of the large stoss ripples on the Namib dune (Ewing et al., 2017) and may have a similar formation mechanism to the slab flows observed on the Maspalomas dune slipface.

4. Discussion

The Namib dune slipface contains an assemblage of aeolian structures bearing a record of the most recent slipface activity. Fresh grainflows have obscured underlying lee slope ripples within the central portion of the barchan slipface while older grainflows are mantled in ripples (Figs. 3 and 5). Evidence of grainfall is scarce in this region of the slipface but more pronounced along the lee slope of the horns (Figs. 2 and 4). Curiosity imaged the Namib dune slipface in late autumn and HiRISE images overlapping with the Curiosity mission indicate that the autumn and winter seasons were a time of little to no slipface advancement for the Namib dune (Bridges et al., 2017). Observations from the rover confirmed there was little grain movement (Bridges et al., 2017) suggesting that any significant grain transport may entirely cease during the autumn and winter seasons. During the summer, the primary wind direction, according to REMS data, ranges from east to south-southwest (Bridges et al., 2017; Newman et al., 2017; Figs. 1 and 7). These winds would be incident to the Namib dune slipface, unfavorable to widespread grainfall generation but potentially conducive to ripple formation and migration on the lee slope as well as the stoss slope (Ewing et al., 2017). Summer, therefore, may be a season of pronounced ripple migration and activation of the secondary slipface

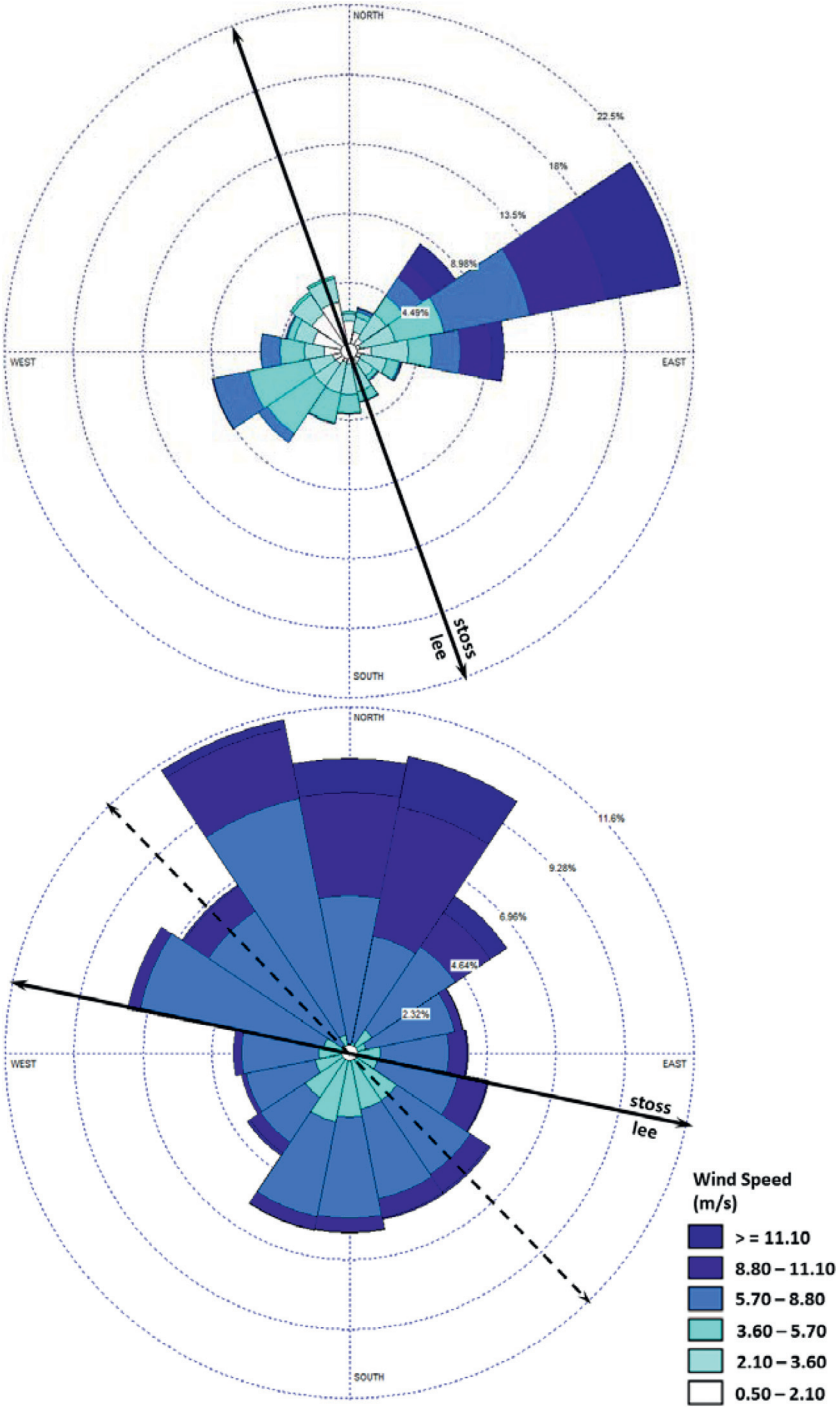

Fig. 7. Wind Regime for the Maspalomas dune field (top) and Gale Crater, Mars (bottom). Data displayed shows seasonal wind patterns at Maspalomas, Gran Canaria, Spain from February–September 2015 and Curiosity REMS wind data (Gomez-Elvira et al., 2012) for sols 884–1485. REMS data was collected along Curiosity's traverse and therefore may include some wind variability due to nearby topographic influences but the general N–S bimodal trend agrees well with mesoscale modelling (e.g. Pla-Garcia et al., 2016). Solid lines represent the orientation of the dune slipface. The dashed line represents the orientation of the large ripples on the stoss slope of the Namib dune, where the migration direction is to the southwest. Ripples on the Maspalomas dune were oriented parallel to the slipface.

along the western flank of the Namib dune. A closer inspection of the patterns of grainflow activity provide more information concerning the aeolian conditions that produced the features on the preserved on the primary and secondary slipface slopes.

4.1. Sediment flux and wind regime

Sediment delivery onto the slipface of a terrestrial dune is largely driven by grainfall, including saltating grains over the dune brink and finer-grained sediment settling further down slope. Patterns of slope failure can be identified within zones on the slipface (e.g. Hunter, 1985; McDonald and Anderson, 1995; Nickling et al., 2002; Sutton et al., 2013a,b; Nield et al., 2017). On terrestrial dunes, there exists a relationship between wind velocity and the location, frequency, and magnitude of grainflows on a slipface. Nield et al. (2017) reported the delivery of sediment to the base of the slipface, where during strong winds ($> 6\,m\,s^{-1}$), a higher number of grainflows occurred, sometimes in clusters of activity, and the grainflows tended to be larger in magnitude in regards to redistributed sediment volume and areal extent. As wind velocities increased, grainflows became capable of delivering sediment to the base of the slipface, thus contributing to the overall advancement the slipface (Nield et al., 2017).

In addition, Nield et al. (2017) observed that larger grainflows initiated at the top of the slipface while smaller grainflows occurred partway down the slipface at greater wind velocities whereas during weaker winds ($< 6\,m\,s^{-1}$), slipface activity consisted of small, thin,

Table 1
Comparison of dune slope and grainflow properties for Earth and Mars recorded in centimeter units. Values in parentheses are the standard deviations for each averaged grainflow morphology. For initiation point, 'U' represents undefined, where the original location of initiation could not be determined. Averaged values are presented for the Maspalomas dune field grainflows from Cornwall et al. (2018). Thickness estimates for the two Namib dune hourglass grainflows were trigonometrically measured using shadow length and the sun's elevation at the time of observation. Average slope for the Namib dune, grainflow length and width was reported by Ewing et al. (2017). The measured hourlgass grainflows on the Namib dune are shown in Fig. 5.

Maspalomas, Morphology	Spain Initiation Point	(Averaged) Upslope Grainflow Thickness	Midpoint Grainflow Thickness	Base Grainflow Thickness	Grainflow Length	Upslope Grainflow Width	Base Grainflow Width	Approx. Area	Slope: 32.15 Estimated Grainflow Volume
Hourglass $n = 29$	31.96	0.522	1.26	2.5	429.711	34.059	93.39	10,978.96	22,494.58
Funnel $n = 9$	156.11	−1.89	−0.42	1.19	313.99	4.99	12.97	189.77	1,312.31
Lobes $n = 26$	218.6	0.38	0.85	1.09	227.21	17.69	36.51	2,882.90	1,944.74
Slab $n = 7$	5.08	0.55	0.79	1.79	684.49	604.32	604.32	424,626.02	182,111.79

Namib Dune, Morphology	Mars Initiation Point	(Measured) Upslope Grainflow Thickness	Midpoint Grainflow Thickness	Base Grainflow Thickness	Grainflow Length	Upslope Grainflow Width	Base Grainflow Width	Approx. Area	Slope: 29 Estimated Grainflow Volume
Hourglass 1	U	U	U	0.45	290	31.41	55.77	16,530.00	1411.559775
Hourglass 2	U	U	U	1.02	600	40.04	59.36	39,600.00	7351.85808
Furrow 1	6.79	U	U	0.32	22.44	0.99	4.56	51.16	5.493240192
Lobe 2b	U	U	U	0.42	29.92	15.15	23.51	578.35	59.11481699
Lobe 3	U	U	U	0.36	24.20	3.03	5.89	71.27	9.76287048

discrete grainflows initiating near the brink with a limited depositional lobe. Observations from the Maspalomas dune field supported these findings (Cornwall et al., 2018) and it is possible that this response also occurs in the Martian environment with wind speeds being adjusted appropriately for Mars atmospheric conditions.

The Namib slipface displays a series of relatively evenly spaced hourglass grainflows with limited occurrences of lobes and funnels (Figs. 2–5). Lobes and funnels did not form as regularly on the Namib dune, compared to observations from Maspalomas, based on their lack of preservation. The lobes and funnels that were identified on the Namib slipface preferentially occurred immediately below the dune brink and were relatively thin, suggesting limited sediment input on to the slipface and a lower frequency of effective wind velocities. Maspalomas lobe and funnel flows were often observed to precede larger hourglass flows (Cornwall et al., 2018). Therefore, it is likely that some lobe and funnel flows were obscured by the larger hourglass grainflows on the Namib dune. However, the lack of evidence of lobe and funnel flows following large grainflows and the concentration of these flows near the dune brink suggests differences in the aeolian environment possibly due to wind speed and direction unconducive to smaller grainflow formation further down the slipface slope.

The two freshest hourglass grainflows on the central portion of the dune were also thinner than the Maspalomas hourglass grainflows and redistributed significantly less volume of sediment compared to terrestrial hourglass grainflows despite having a greater planform area (Table 1). Terrestrial hourglass grainflows were highly variable in the amount of sediment redistributed for each grainflow due to variability in area (Table 1; Fig. 9) and the Namib dune may also have high variability in grainflow area (Figs. 2–4). In addition, when compared to other older grainflows on the Namib slipface, the two measured (and freshest) hourglass grainflows may be smaller than typical Mars grainflows and may have formed in response to slope destabilization from slumping (Figs. 3 and 5). The difference in martian grainflow thickness of lobe, funnel and hourglass grainflows compared to terrestrial grainflows may be characteristic of all grainflows on Mars. Slopes may be more easily destabilized with less sediment load due to the lower surface gravity and its effect on grain packing. However, more measurements of martian grainflow thicknesses and attributes of grain

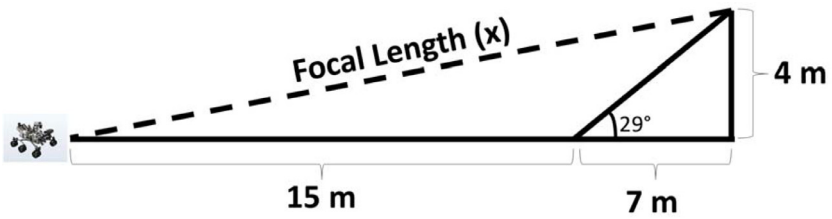

$$\text{Resolution at Brink} = 2\tan^{-1}\left(\frac{{}^{1}/_{2}Height}{Distance\ to\ Brink}\right)$$

$$(\text{Focal Length})^2 = (\text{Distance to Brink})^2 + (\text{Height})^2$$

$$\text{Scale Factor} = \frac{Resolution\ at\ Brink}{Focal\ Length}$$

Fig. 8. Schematic showing calculations for measurements on the Namib dune using spatial analysis techniques to account for perspective foreshortening. The scale factor near the top of the dune above the two hourglass grainflows in Fig. 5 was determined to be ~1.904.

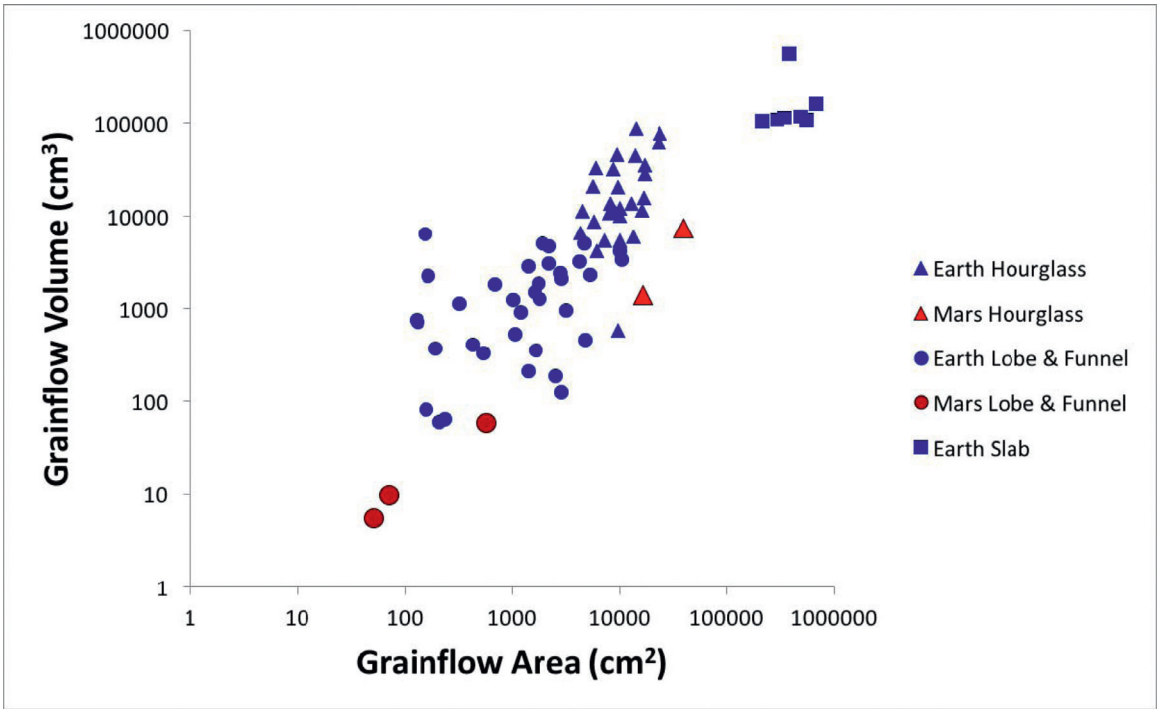

Fig. 9. Mars (red) and Maspalomas (blue) grainflow estimations of area vs volume on log-log axes. Hourglass flows are shown as triangles, lobe and funnel flows are shown as circles, and slab flows are shown as boxes. (For interpretation of the references to colour in this figure legend, the reader is referred to the web version of this article.).

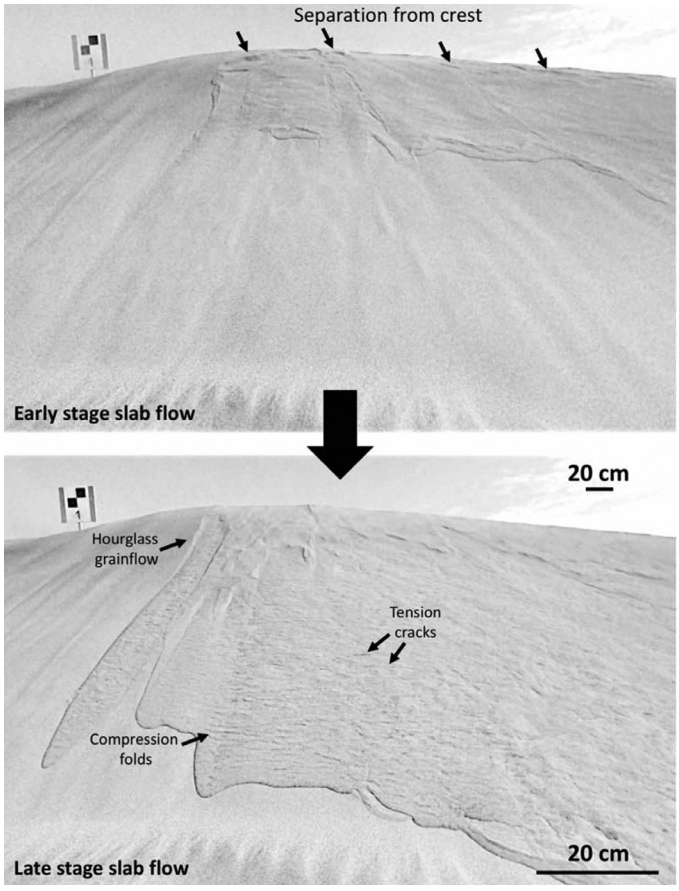

Fig. 10. Formation of a slab flow (top) in the Maspalomas dune field, Gran Canaria, Spain. Early stage slab flow formation begins as a series of horizontal tensional cracks a few centimeters below the dune crest shortly followed by sediment flow downslope. Late stage slab flow (bottom) contains multiple compression folds as well as tensional cracks throughout the flow surface. Secondary grainflow may also be initiated due to nearby slope destabilization such as the hourglass flow on the left. The time lapse between the early stage and late stage slab flow images is 11 seconds. Two scale bars are given to account for perspective.

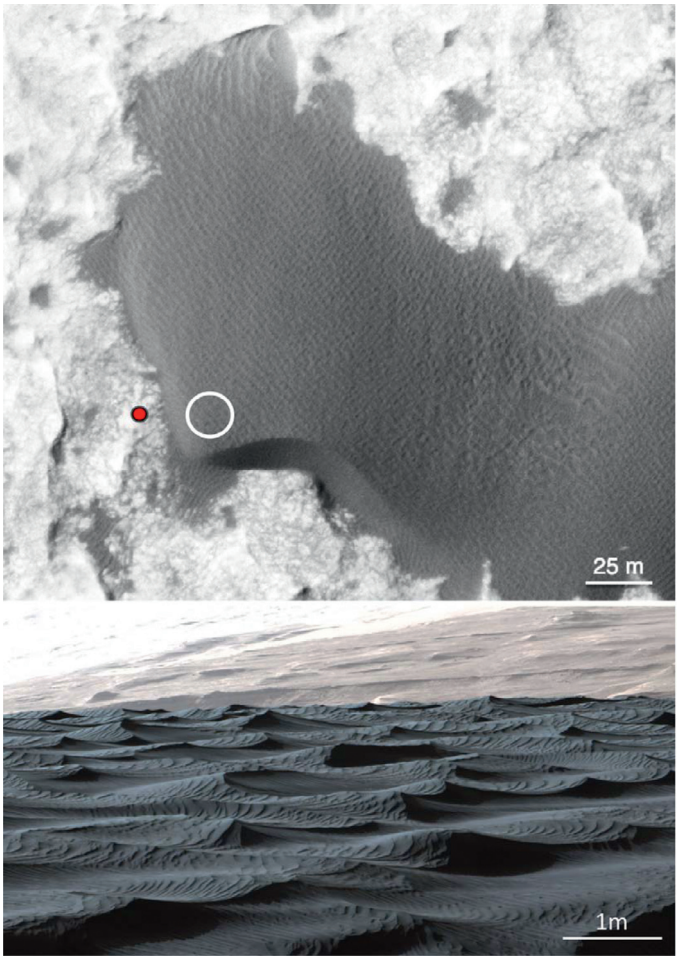

Fig. 11. Namib dune as seen from HiRISE satellite image ESP_018920_1755 (top) and the large stoss ripples as seen from Curiosity (bottom). Red dot indicates the location of the Curiosity rover when the bottom image was taken by the mastcam (MCAM05410) on sol 1192 of the mission. The large ripples are actively migrating on the stoss slope and obliquely intersect the dune crest line, potentially introducing significant amounts of sediment on to the slipface thus triggering large grainflows.

texture related to angle of repose are required for a more definitive conclusion.

Any grainfall that may have occurred on the Namib dune slipface during the most recent aeolian activity appears to be ineffective at erasing previous grainflow events with the exception of the lee slopes of the barchan horns, where some infilling of alcoves has occurred (Figs. 2 and 4). Under terrestrial conditions, grainfall rapidly erases previous slipface activity and restores the slipface to a critical angle of repose, resulting in a continuous cycle of avalanching and slope restoration (e.g. Bagnold, 1941; Allen, 1970; Hunter, 1985; Anderson, 1988; McDonald and Anderson, 1995; Nickling et al., 2002; Cupp et al., 2005; Sutton, 2012; Sutton et al., 2013a,b). On the central portion of the Namib dune, there is very little evidence of grainfall or any kind of sediment redistribution following the most recent grainflow activity (Ewing et al., 2017; Fig. 3). Outside of the central portion of the dune slipface, grainfall appears limited to the upper slopes of the slipface (Figs. 2, 4, and 5) and portions of the dune apron, likely as a result of along slope transport from an easterly wind direction, where grainfall was preferentially deposited on west-facing slopes of hourglass grainflow alcoves and small, incipient ripples formed on east-facing slopes (Ewing et al., 2017).

It is likely that sediment delivery to the slipface via grainfall is intermittent or punctuated at certain times of the martian year based on seasonal changes of the wind direction and magnitude (Fig. 7). The absence of smaller grainflows on the mid slope suggest that the grainfall zone for the most recent grainflow event was limited to the uppermost part of the Namib dune, suggesting low velocity winds (Nield et al., 2017; Cornwall et al., 2018). However, the existence of older, larger hourglass grainflows testifies of greater wind velocities which are required to supply the sediment load necessary to initiate these flows and successfully transport sediment to the base of the lee slope (Nield et al., 2017). It is possible that small grainflows do not form on the mid slope of the Namib slipface in any season if grainfall and saltation lengths are ineffective at causing mid slope over steepening. Alternatively, smaller grainflows may have been overridden by larger flows from a previous, more energetic event and the most recent grainflow activity may be the result of SE winds from the summer season.

4.2. Tensional cracks

Slab flows in the Maspalomas dune field initially manifested as a series of horizontal tensional cracks that ran parallel to the dune brink (Figs. 9 and 10; Table 1; Cornwall et al., 2018). While slab flows have not been extensively studied, there are a number of factors that may influence the formation of these large grainflows on Earth, including the presence of liquid water, ice, or salt (McKee et al., 1971; McKee and Bigarella, 1972; Morris et al., 1972; Bigarella, 1975), complex airflow patterns that affect sediment deposition (McDonald and Anderson, 1995; Nickling et al., 2002; Cupp et al., 2005), or slump degeneration and dry cohesion (Fryberger and Schenk, 1981; Sutton et al., 2013b).

The presence of complex airflow patterns having a significant impact on slab formation, where the most recent seasonal winds are likely

from the southeast, seems unlikely. The Namib dune slipface has multiple tensional cracks near the dune crest on the central portion of the dune and also exhibits a break in slope (Fig. 5a) that is not present elsewhere on the slipface (Fig. 2 and 4). This break in slope may have been a slab flow in progress which was halted possibly due to sediment cohesion from ice or geochemical precipitates or lack of sufficient sediment load to keep the flow moving to the base of the slipface. Induration from ice or geochemical precipitates may be common on martian dunes (e.g. Malin and Edgett, 2001; Bourke, 2004; Bourke, 2005; Fenton et al., 2005; Schatz et al., 2006, Bourke et al., 2008; Gardin et al., 2011). Small amounts of cements such as salt in aeolian deposits can greatly affect threshold shear velocity (Nickling and Ecclestone, 1981) and therefore also impede the initiation and subsequent mobility of grainflows, causing the cessation of slipface advancement during autumn and winter. However, an extremely low volatile content was measured at the Namib dune during late autumn (e.g. Ehlmann et al., 2017) and the only crystalline sulfate mineral present was anhydrite at less than 1.5 wt.% (Achilles et al., 2017). Therefore, it seems more likely that the slump feature may have halted due to lack of momentum.

4.3. Stoss ripple migration and grainflow initiation

An alternative mechanism to grainflow initiation from lee slope oversteepening due to grainfall may occur on the Namib dune at certain periods throughout the martian year and may influence the formation of larger hourglass grainflows. The Bagnold dunes are actively migrating at an estimated rate of 0.75 m per Mars year (Silvestro et al., 2013). Superimposed on top of these dunes are large ripples, having a height of 10 cm and spacing between 1 to 2 m (Lapotre et al., 2016; Ewing et al., 2017). These ripple height estimates are likely a lower boundary estimate because measurements were performed at the base of the secondary lee slope of the Namib dune (Lapotre et al., 2016; Ewing et al., 2017), where ripple wavelengths and heights are generally smaller compared to ripples on the stoss slope. The large stoss ripples migrate at a faster rate of approximately 1.27 m per Mars year as measured from a similar barchan dune southwest of Namib dune (Silvestro et al., 2013). The large stoss ripples intersect the Namib dune crest obliquely (Fig. 11) along the slopes of the barchan horns and transversely along the central slipface (Ewing et al., 2017), resulting in an undulating morphology at the dune brink (Figs. 2–5). The occurrence of hourglass grainflow events on the Namib dune may be augmented by the migration of these large stoss ripples, especially during times of the martian year when winds have a more easterly or westerly component (Fig. 7). As the stoss ripples intersect the dune brink, sediment spills on to the upper slopes of the slipface, creating localized over steepening without grainfall, similar to the migration of terrestrial dunes on draas (Bagnold, 1941; Cooke and Warren, 1973; Ewing et al., 2017). This would result in periodic grainflows along the slipface slopes during seasons of otherwise inactivity but may not be substantial enough to foster significant slipface advancement.

It is possible that this mechanism of grainflow initiation via ripple migration was active during the summer season when the southeasterly winds were more active. High magnitude northerly winds have the potential to produce grainfall and grain saltation over the entire dune slipface. Without northerly winds to transport sediment on to the slipface, there would be very little grainfall to restore the slipface for subsequent grainflow activity, especially along the central portion of the slipface. Therefore, if ripple migration does influence grainflow activity, the process would eventually terminate, leaving behind a few fresh grainflows and very little evidence of grainfall, or slope restoration. This might explain how the Namib dune continues to advance during the summer season, as evidenced by HiRISE monitoring (Bridges et al., 2017), despite wind conditions being contrary to dune orientation and unconducive to grainfall. The older hourglass grainflows mantled in impact ripples may be the product of this process which is likely ongoing throughout the summer. Once formed, the grainflows would be subject to sediment redistribution from the SE winds, creating impact ripples across the slope but these winds would ultimately be ineffective at restoring the slipface compared to northerly winds that generate extensive grainfall. In addition, sediment deposition on to the slipface from ripple migration might also explain why Curiosity images from late autumn showed little evidence of grainfall deposits and smaller grainflows that preferentially formed just below the brink (Figs. 2–5).

4.4. Seasonal activity

With little evidence of pervasive slope rebuilding from grainfall in the images captured by the Curiosity rover, it is likely that slipface activity on Mars occurs in stages throughout the martian year, similar to the seasonal migration observed at the Nili Patera dune field (Ayoub et al., 2014) or the seasonal erosion and rebuilding observed in polar dunes on Mars (Hansen et al., 2011). Local wind magnitude and direction changes drastically throughout the martian year (Fig. 7) and grainflow activity and slope rebuilding may be controlled by these seasonal changes (e.g. Newman et al., 2017; Bridges et al., 2017).

There may be a season of prolonged ripple migration, where winds have a more eastern or western component, such as the summer. Under these conditions, sediment may be regularly introduced on to the slipface via large stoss ripples that intersect the dune brink obliquely and grainfall may be confined to the lee slope of the horns (Ewing et al., 2017). Lobe and funnel flows most likely preferentially form just below the dune brink due to the seasonal wind direction, which is incapable of transporting sufficient sediment for over steepening on the mid slope region. Winds incident or oblique to the slipface may be conducive to ripple migration and lateral sediment transport but may not be sufficient for rebuilding the slipface slope for subsequent grainflow, where additional sediment input may be required to achieve a critical angle of repose. It is possible that during periods when the wind directions are more easterly or westerly, grainflow recurrence becomes more punctuated and may cease completely until northern winds resume and restore the slipface.

During northerly wind events, there may be more widespread grainfall and regular grainflow activity, including lobe and funnel flow initiation mid slope as opposed to just below the dune brink. Slope restoration may also be enhanced by complex airflow patterns, such as airflow diversion around the barchan dune resulting in lateral transport to the east (e.g. Ewing et al., 2017), capable of further redistribution of sediment across the slipface. Future investigations involving seasonal airflow modelling may be able to resolve some of these seasonal wind patterns that potentially play a crucial role in slope restoration and grainflow initiation at the Namib dune and other dunes on Mars.

4.5. Implications for the martian rock record

Due to the thin nature of the grainflows preserved on the Namib dune, the recognition or preservation of grainflows in the martian rock record may be difficult. The Stimson formation is composed of cross-bedded sandstones and located near the base of Aeolis Mons (Mount Sharp) and has been determined to be a record of a dry-aeolian dune system (Banham et al., 2018). While many aeolian structures have been identified such as wind ripple stratifications and compound dune bedforms, within cross-sets, there has been no conclusive evidence of grainflow strata (Banham et al., 2018). The absence of grainflow structures in the Stimson formation may be due to reworking of the lee slope by migrating ripples which appear to occur regularly on the Namib dune (Eastwood et al., 2012; Lapotre et al., 2016; Ewing et al., 2017; Banham et al., 2018). If the thinness of grainflow deposits on the Namib dune is typical of martian aeolian environments, grainflows may be rapidly erased or reworked before preservation can take place.

Alternatively, the lack of grainflow strata may not be representative

of all martian aeolianites and may be heavily influenced by changes in the planet's obliquity. Wind directions are little affected by orbital changes while wind speeds can vary significantly and may have a great impact on aeolian activity (Fenton and Richards, 2001). Aeolianites that contain grainflow strata could be representative of dunes that formed under high obliquity when winds speeds are greater and aeolian activity more consistent. Under these conditions, grainflows would be quickly buried by grainfall and preserved as opposed to being reworked by wind ripples. In addition, greater wind speeds would result in a higher sediment flux, increasing grainflow frequency and potentially the grainflow thickness, thereby increasing the probability of preservation in the rock record. During periods of greater obliquity, seasonal variations in slipface activity may also be preserved. For example, early spring is more conducive to grainflow activity and slipface advancement for the Namib dune, while the southeast summer winds promote ripple formation and migration on the stoss and lee slopes (Bridges et al., 2017; Ewing et al., 2017). Under a more active aeolian environment, these seasonal cycles may be well preserved in the martian rock record.

5. Conclusion

The aeolian structures preserved on the Namib dune on Mars are very similar to terrestrial slipface features. However, the level of preservation for each grainflow, ripple, and tensional crack on the Namib dune suggests that grainfall contributed very little to slipface reworking at the time the Curiosity rover visited the dune. Based on terrestrial observation, sediment input from the stoss slope is essential for the formation of larger grainflows, such as hourglass flows, because they are typically initiated by localized slope oversteepening just below the dune brink from saltating sediment delivered from the stoss slope (e.g. Allen, 1968; Allen, 1970; Borowka, 1979; Hunter, 1985; Anderson, 1988; McDonald and Anderson, 1992; McDonald and Anderson, 1995; Nickling et al., 2002; Walker and Nickling, 2002; Cupp et al., 2005; Kok et al., 2012; Sutton, 2012; Sutton et al., 2013a,b). Therefore, evidence of deposition from saltation or suspension settling is expected with the presence of hourglass grainflows but is limited to the lee slopes of the horns on the Namib dune slipface. In addition, the formation of small lobe and funnel grainflows just below the dune brink also suggests a wind environment incapable of sediment delivery further downslope.

The Curiosity rover visited the Namib dune late autumn, during a time of low aeolian activity (Bridges et al., 2017). Prior to the autumn season, winds were predominantly from the southeast, obliquely incident to the dune slipface. These winds would be ineffective at generating grainfall across the entire Namib dune slipface but conducive to stoss ripple migration. An additional source of sediment, potentially triggering grainflow activity under winds contrary to dune orientation, may be from the sediment deposited from large stoss ripples on the Namib dune that intersect the dune brink obliquely during migration. The advancement of these large ripples would regularly deposit sediment on to the slipface and the most recent slipface activity may have been generated under this mechanism of sediment transport which would explain slipface advancement throughout the summer season as seen from HiRISE-based monitoring (Bridges et al., 2017) and the existence of a series of hourglass grainflows with little indication of grainfall deposition as well as lobe funnel flows confined to just below the dune brink.

This study has significant implications for understanding modern aeolian dynamics including mechanisms for slipface advancement, dune migration rates, and interpretations of sedimentary structures on Earth, Mars, and other bodies with aeolian deposits. The presence or absence of grainflow strata in martian aeolianites potentially suggests times of high and low obliquity. Changes in obliquity have a substantial impact on aeolian processes (Fenton and Richardson, 2001), potentially affecting the types of aeolian structures that are preserved in the rock record. The study of recent grainflows and other aeolian structures directly impact our understanding of aeolianites such as those found at Meridiani Planum (Grotzinger et al., 2005) as well as the aeolian crossbeds of Aeolis Mons (HYPERLINK \l "bib8" Banham et al., 2018) and may provide valuable insights into the paleoenvironments in which they formed.

Acknowledgements

We would like to thank Ryan Ewing and Mathieu Lapotre for their very helpful comments, edits, and suggestions for this paper. This research was funded by the Vice Chancellor's Research Scholarship, University of Ulster and the Natural Environment Research Council grant NE/F019483/1. MCB's contribution was supported in part by EU FP7 CIG #618892.

References

Achilles, C.N., et al., 2017. Mineralogy of active eolian sediment from the Namib Dune, Gale Crater, Mars. J. Geophys. Res. Planets 122, 2344–2361.
Allen, J., 1968. The diffusion of grains in the lee of ripples, dunes and sand deltas. J. Sediment. Petrol. 38 (2), 621–633. http://dx.doi.org/10.1306/74D719FB-2B21-11D7-8648000102C1865D.
Allen, J., 1970. The avalanching of granular solids on dune and similar slopes. J. Geol. 78, 326–351.
Almeida, M.P., Parteli, E.J.R., Andrade, J.S., Herrmann, H.J., 2008. Giant saltation on Mars. Proc. Natl. Acad. Sci. USA 105, 6222–6226.
Anderson, R., 1988. The pattern of grainfall deposition in the lee of aeolian dunes. Sedimentology 35 (2), 175–188. http://dx.doi.org/10.1111/j.1365-3091.1988.tb00943.x.
Anderson, F.S., Greeley, R., Xu, P., Lo, E., Blumberg, D.G., Haberle, R.M., Murphy, J.R., 1999. Assessing the Martian surface distribution of aeolian sand using a Mars general circulation model. J. Geophys. Res. 104, 18991–19002.
Ayoub, F., Avouac, J.-P., Newman, C.E., Richardson, M.I., Lucas, A., Leprince, S., Bridges, N.T., 2014. Threshold for sand mobility on Mars calibrated from seasonal variations in sand flux. Nature Comm. 5, 5096. http://dx.doi.org/10.1038/ncomms6096.
Bagnold, R., 1941. The Physics of Blown Sand and Desert Dunes. Methuen, London, pp. 265.
Banham, S., Gupta, S., Rubin, D., Watkins, J., Edgett, K.S., Sumner, D.Y., Grotzinger, J.P., Lewis, K., Edgar, L., Stack, K., Barnes, R., Bell III, J., Day, M.D., Ewing, R.C., Lapotre, M.G.A., Stein, N., Rivera-Hernandez, F., Vasavada, A., 2018. Ancient Martian aeolian processes and palaeogeomorphology reconstructed from the Stimson formation on the lower slope of Aeolis Mons, Gale crater, Mars. Sedimentology. http://dx.doi.org/10.1111/sed.12469.
Bigarella, J.J., 1975. Structures developed by dissipation of dune and beach ridge deposits. CATENA 2, 107–152.
Borówka, R.K., 1979. Accumulation and redeposition of eolian sands on the lee slopes of dunes and their influence on formation of sedimentary structures. Quaest. Geographicae 5, 5–22.
Bourke, M.C., 2004. Niveo-aeolian and denivation deposits on Mars, EOS. Transactions, Fall Meeting, Suppl. 85 (46) ABS P21B-01.
Bourke, M.C., 2005. Alluvial fans on dunes in Kaiser Crater suggest niveo-aeolian and denivation processes on Mars. Lunar Planet. Sci. XXXVI Abs #2373.
Bourke, M.C., Edgett, K.S., Cantor, B.A., 2008. Recent aeolian dune change on Mars. Geomorphology 94, 247–255.
Bourke, M.C., Ewing, R.C., Finnegan, D., McGowan, H.A., 2009b. Sand dune movement in the Victoria Valley, Antarctica. Geomorphology 109, 148–160. http://dx.doi.org/10.1016/j.geomorph.2009.02.028.
Breton, C., Lancaster, N., Nickling, W.G., 2008. Magnitude and frequency of grain flows on a desert sand dune. Geomorphology 95 (3-4), 518–523. http://dx.doi.org/10.1016/j.geomorph.2007.07.004.
Bridges, N.T., Geissler, P.E., McEwen, A.S., Thomson, B.J., Chuang, F.C., Herkenhoff, K.E., Keszthelyi, L.P., Martinez-Alonso, S., 2007. Windy Mars: a dynamic planet as seen by the HiRISE camera. Geophys. Res. Lett. 34.
Bridges, N.T., Bourke, M.C., Geissler, P.E., Banks, M.E., Colon, C., Diniega, S., Golombek, M.P., Hansen, C.J., Mattson, S., McEwen, A.S., Mellon, M.T., Stantzos, N., Thomson, B.J., 2011. Planet-wide sand motion on Mars. Geology 40, 31–34.
Bridges, N.T., et al., 2012a. Planet-wide sand motion on Mars. Geology 40, 31–34.
Bridges, N.T., Ayoub, F., Avouac, J.-P., Leprince, S., Lucas, A., Mattson, S., 2012b. Earth-like sand fluxes on Mars. Nature 485, 339–342.
Bridges, N.T., Geissler, P.E., Silvestro, S., Banks, M.E., 2013. Bedform migration on Mars: current results and future plans. Aeolian Res. 9, 133–151.
Bridges, N.T., et al., 2016. Investigation of the Bagnold dunes by the Curiosity rover: overview of initial results from the first study of an active dune field on another planet. In: 47th LPSC, abs. 2298.
Bridges, N.T., Sullivan, R., Newman, C.E., Navarro, S., van Beek, J., Ewing, R.C., Ayoub, F., Silvestro, S., Gasnault, O., Le Mouelic, S., Lapotre, M.G.A., Rapin, W., 2017. Martian aeolian activity at the Bagnold Dunes, Gale Crater: The view from the surface and orbit. JGR Planets 122, 2077–2110.
Bristow, C.S., Lancaster, N., 2004. Movement of a small slipfaceless dome dune in the Namib Sand Sea, Namibia. Geomorphology 59, 189–196. http://dx.doi.org/10.1016/

j.geomorph.2003.09.015.
Cardinale, M., Komatsu, G., Silvestro, S., Tirsch, S., 2012. The influence of local topography for wind direction on Mars: two examples of dune fields in crate basins. Earth Surf. Process. Landforms 37, 1437–1443.
Cardinale, M., Silvestro, S., Vaz, D.A., Michaels, T., Bourke, M.C., Komatsu, G., Marinangeli, L., 2016. Present-day aeolian activity in Herschel Crater, Mars. Icarus 265, 139–148.
Chojnacki, M., Burr, D.M., Moersch, J.E., Michaels, T.I., 2011. Orbital observations of contemporary dune activity in Endeavor crater, Meridiani Planum, Mars. J. Geophys. Res. 116http://dx.doi.org/10.1029/2010JE003675. EooF19.
Chojnacki, M., Johnson, J.R., Moersch, J.E., Fenton, L.K., Michaels, T.I., Bell, J.F., 2015. Persistent aeolian activity at Endeavour crater, Meridiani Planum, Mars; new observations from orbit and the surface. Icarus 251, 275–290.
Claudin, P., Andreotti, B., 2006. A scaling law for aeolian dunes on Mars, Venus, Earth, and for subaqueous ripples. Earth Planet. Sci. Lett. 252, 30–44.
Cooke, R., Warren, A., 1973. Geomorphology in Deserts. B. T. Batsford, Ltd., London.
Cornwall, C., Jackson, D.W.T., Bourke, M.C., Cooper, J.A.G., 2018. Morphometric analysis of slipface processes of an aeolian dune: implications for grainflow dynamics. Sedimentology. http://dx.doi.org/10.1111/sed.12456.
Cousin, A., et al., 2017. Geochemistry of the Bagnold Dune Field as observed by ChemCam, and comparison with other aeolian deposits at Gale Crater. J. Geophys. Res. Planets 122, 2144–2162.
Cupp, K., Lancaster, N., Nickling, W.G., 2005. Lee slope processes on a small artificial flow-transverse dune. Eos Trans. Am. Geophys. Union 86 (52, Fall Meeting Supplement) Abs #H51C-0386.
Curran, P., 1985. Principles of Remote Sensing. Longman, pp. 282.
Dasgupta, P., Manna, P., 2011. Geometrical mechanisms of inverse grading in grain-flow deposits: an experimental revelation. Earth-Sci. Rev. 104 (1-3), 186–198.
Dong, Z., Wang, X., Chen, G., 2000. Monitoring sand dune advance in the Taklimakan Desert. Geomorphology 35, 219–231. http://dx.doi.org/10.1016/ S0169-555X(00)00039-8.
Eastwood, E.N., Kocurek, G., Mohrig, D., Swanson, T., 2012. Methodology for reconstructing wind direction, wind speed, and duration of wind events from aeolian cross-strata. JGR 117, F03035. http://dx.doi.org/10.1029/2012JF002368.
Ehlmann, B.L., et al., 2017. Chemistry, mineralogy, and grain properties at Namib and High Dunes, Bagnold Dune Field, Gale Crater, Mars: a synthesis of Curiosity Rover observations. J. Geophys. Res. Planets 122. http://dx.doi.org/10.1002/2017JE005267.
Ewing, R. C., M. G. A. Lapotre, K. W. Lewis, M. Day, N. Stein, D. M. Rubin, R. Sullivan, S. Banham, M. P. Lamb, N. T. Bridges, S. Gupta, and W. W. Fischer (2017) Sedimentary processes of the Bagnold Dunes: implications for the eolian rock record of Mars, 122, 2544–2573.
Fenton, L.K., Richardson, M.I., 2001. Martian surface winds: insensitivity to orbital changes and implications for aeolian processes. J. Geophys. Res. 106, 32885–32902.
Fenton, L.K., Toigo, A.D., Richardson, M.I., 2005. Aeolian processes in Proctor Crater on Mars: mesoscale modeling of dune-forming winds. J. Geophys. Res. (Planets) 110, E06005.
Fenton, L., 2006. Dune migration and slip face advancement in the Rabe Crater dune field, Mars. Geophys. Res. Lett. 33.
Finkel, H.J., 1959. The barchans of southern Peru. J. Geol. 67, 614–647. http://dx.doi.org/10.1086/626622.
Fryberger, S.G., Schenk, C., 1981. Wind sedimentation tunnel experiments on the origins of aeolian strata. Sedimentology 28 (6), 805–821. http://dx.doi.org/10.1111/j.1365-3091.1981.tb01944.x.
Gardin, E., Bourke, M.C., Allemand, P., Quantin, C., 2011. High albedo dune features suggest past dune migration and possible geochemical cementation of aeolian sediments on Mars. Icarus 212 (2), 590–596.
Geissler, P.E., Stantzos, N.W., Bridges, N.T., Bourke, M.C., Silvestro, S., Fenton, L.K., 2013. Shifting sand on Mars: insights from tropical intra-crater dunes. Earth Surf. Processes Landforms 48, 407–412.
Gomez-Elvira, J., et al., 2012. REMS: the environmental sensor suite for the Mars Science Laboratory rover. Space Sci. Rev. 170 (1-4), 583–640.
Greeley, R., 2002. Saltation impact as a means for raising dust on Mars. Planet. Space Sci. 50, 151–155.
Greeley, R., Iversen, J.D., 1985. Wind as a geological process on Earth, Mars and Venus. Cambridge Planetary Science Series. Cambridge Univ. Press, pp. 78–79.
Grotzinger, J., Arvidson, R., Bell, J., Calvin, W., Clark, B., Fike, D., Golombek, M., Greeley, R., Haldemann, A., Herkenhoff, K., Jolliff, B., Knoll, A., Malin, M., McLennan, S., Parker, T., Soderblom, L., Sohl-Dickstein, J., Squyres, S., Tosca, N., Watters, W., 2005. Stratigraphy and sedimentology of a dry to wet eolian depositional system, Burns formation, Meridiani Planum, Mars. Earth Planet. Sci. Lett. 240 (1), 11–72.
Haberle, R.M., Murphy, J.R., Schaeffer, J., 2003. Orbital change experiments with a Mars general circulation model. Icarus 161, 66–89.
Hansen, C.J., Bourke, M.C., Bridges, N.T., Byrne, S., Colon, C., Diniega, S., Dundas, C., Herkenhoff, K., McEwen, A., Mellon, M., Portyankina, G., Thomas, N., 2011. Seasonal erosion and restoration of Mars' northern polar dunes. Science 331 (6017), 575–578.
Hastenrath, S.L., 1967. The barchans of the Arequipa region, southern Peru. Z. Geomorphol. 11, 300–311.
Hayward, R.K., Mullins, K.F., Fenton, L.K., Hare, T.M., Titus, T.N., Bourke, M.C., Colaprete, A., Christensen, P.R., 2007. Mars Global Digital Dune Database and initial science results. J. Geophys. Res 112.
Hayward, R.K., Titus, T.N., Michaels, T.I., Fenton, L.K., Colaprete, A., Christensen, P.R., 2009. Aeolian dunes as ground truth for atmospheric modeling on Mars. J. Geophys. Res. 114.
Hernandez, L., Alonso, I., Ruiz, P., Perez-Chacon, E., Suarez, C., Alcantara-Carrio, J., 2002. Decadal environmental changes on the dune field of Maspalomas (Canary Islands): evidences of an erosive tendency. In: Gomes, F.Veloso, Pinto, F.Taveira, Das Neves, L. (Eds.), Littoral 2002: The Changing Coast, vol. 3. Samara Publishing Limited, Cardigan, UK, pp. 293–297.
Hobbs, S.W., Paull, D.J., Bourke, M.C., 2010. Aeolian processes and dune morphology in Gale crater. In: Proceedings, Lunar Planetary Science Conference. XLI Abs. #1561.
Huertas, A., Nevatia, R., 1988. Detecting buildings in aerial images, computer vision. Graphics Image Process. 41, 131–152.
Hunter, R.E., 1977. Basic types of stratification in small eolian dunes. Sedimentology 24, 361–387. http://dx.doi.org/10.1111/j.1365-3091.1977.tb00128.x.
Hunter, R., 1985. A kinematic model for the structure of lee-side deposits. Sedimentology 32, 409–422.
Jackson, D.W.T., Beyers, J.H.M., Delgado-Fernandez, I., Baas, A.C.W., Cooper, J.A.G., Lynch, K., 2013a. Airflow reversal and alternating corkscrew vortices in foredune wake zones during perpendicular and oblique offshore winds. Geomorphology 187, 86–93.
Jackson, D., Cruz-Avero, N., Smyth, T., Hernandez-Calvento, L., 2013b. 3D airflow modeling and dune migration patterns in an arid coastal dune field. J. Coastal Res. 65, 1301–1306.
Jackson, D.W.T., Bourke, M.C., Smyth, T., 2015. The dune effect on sand-transporting winds on Mars. Nature Commun. 6, 8796.
Jimenez, J.A., Maia, L.P., Serraà, J., Morais, J., 1999. Aeolian dune migration along the Ceara coast, north-eastern Brazil. Sedimentology 46, 689–701. http://dx.doi.org/10.1046/j.1365-3091.1999.00240.x.
Johnson, J.R., et al., 2017. Visible/near-infrared spectral diversity from in situ observations of the Bagnold Dune Field sands in Gale crater, Mars. J. Geophys. Res. Planets 122. http://dx.doi.org/10.1002/2016JE005187.
Kok, J.F., 2010a. An improved parameterization of wind-blown sand flux on Mars that includes the effect of hysteresis. Geophys. Res. Lett. 37, L12202. http://dx.doi.org/10.1029/2010GL043646.
Kok, J.F., 2010b. Difference in the wind speeds required for initiation versus continuation of sand transport on Mars: implications for dunes and dust storms. Phys. Rev. Lett. 104, 074502.
Kok, J.F., Parteli, E.J.R., Michaels, T.I., Bou Karam, D., 2012. The physics of wind-blown sand and dust. Rep. Prog. Phys. 75, 106901.
Lapotre, M., et al., 2016. Large wind ripples on Mars: a record of atmospheric evolution. Science 353, 55–58.
Lapotre, M.G.A., Ehlmann, B.L., Minson, S.E., Arvidson, R.E., Ayoub, F., Fraeman, A.A., Ewing, R.C., Bridges, N.T., 2017. Compositional variations in sands of the Bagnold Dunes, Gale Crater, Mars, from visible-shortwave infrared spectroscopy and comparison with ground truth from the Curiosity rover. J. Geophys. Res. Planets 122. http://dx.doi.org/10.1002/2016JE005133.
Liow, Y.T., Pavlidis, T., 1990. Use of shadows for extracting buildings in aerial images. Comput. Vision Graphics Image Process 49242–49277.
Long, J.T., Sharp, R.P., 1964. Barchan-dune movement in Imperial Valley, California. Geol. Soc. Am. Bull. 75, 149–156.
Malin, M.C., Edgett, K.S., 2001. The Mars global surveyor Mars orbiter camera: interplanetary cruise through primary mission. J. Geophys. Res. (Planets) 106 (E10) 23,429-23,570.
Martinez, J., 1986. Dunas de Maspalomas (Gran Canaria): naturaleza petrologica de sus arenas. Anuario de Estudios Atlanticos 32, 785–794.
Marzol, M., 1987. Las Precipitaciones en las Islas Canarias. Servicio de Publicaciones de la Universidad de La Laguna, Santa Cruz de Tenerife, Spain, pp. 220.
McDonald, R., Anderson, R., 1992. The morphology and dynamics of natural and laboratory grain flows. In: Lutes, L.D., Niedzwecki, J.M. (Eds.), Engineering Mechanics: Proceedings of the 9th Conference. New York. A. S. C. E., pp. 748–751.
McDonald, R., Anderson, R., 1995. Experimental verification of aeolian saltation and lee side deposition models. Sedimentology 42 (1), 39–56. http://dx.doi.org/10.1111/j.1365-3091.1995.tb01270.x.
McDonald, R., Anderson, R., 1996. Constraints on eolian grain flow dynamics through laboratory experiments on sand slopes. J. Sed. Res. 66 (3), 642–653.
McKee, E.D., Douglass, J.R., Rittenhouse, S., 1971. Deformation of lee-side laminae in eolian dunes. Geol. Soc. Am. Bull. 82 (2), 359–378.
McKee, E.D., Bigarella, J.J., 1972. Deformational structures in Brazillian coastal dunes. J. Sediment. Res. 42 (3), 670–681.
Morris, E.C., Mutch, T.A., Holt, H.E., 1972. Atlas of geological features in the dry valleys of South Victoria Land. Antarctica 52 U.S. Geological Survey Interagency report: Astrogeology.
Newman, C.E., Gomez-Elvira, J., Marin, M., Navarro, S., Torres, J., Richardson, M.I., Battalio, J.M., Guzewich, S.D., Sullivan, R., de la Torre, M., Vasavada, A.R., Bridges, N.T., 2017. Winds measured by the Rover Environmental Monitoring Station (REMS) during the Mars Science Laboratory (MSL) rover's Bagnold Dunes Campaign and comparison with numerical modeling using MarsWRF. Icarus 291, 203–231.
Merrison, J.P., Gunnlaugsson, H.P., Nornberg, P., Jensen, A.E., Rasmussen, K.R., 2007. Determination of the wind induced detachment threshold for granular material on Mars using wind tunnel simulations. Icarus 191 (2), 568–580.
Nield, J.M., Wiggs, G.F.S., Baddock, M.C., Hipondoka, M.H.T., 2017. Coupling leeside grainfall to avalanche characteristics in aeolian dune dynamics. Geology 45 (3), 271–274. http://dx.doi.org/10.1130/G38800.1.
Nickling, W.G., Ecclestone, M., 1981. The effects of soluble salts on the threshold shear velocity of fine sand. Sedimentology 28 (4), 505–510.
Nickling, W.G., 1988. The initiation of particle movement by wind. Sedimentology 35 (3), 499–511.
Nickling, W.G., Neuman, C.M., Lancaster, N., 2002. Grainfall processes in the lee of transverse dunes, Silver Peak, Nevada. Sedimentology 49 (1), 191–209. http://dx.doi.org/10.1046/j.13653091.202.00443.x.

O'Connell-Cooper, C.D., Spray, J.G., Thompson, L.M., Gellert, R., Berger, J.A., Boyd, N.I., Desouza, E.D., Perrett, G.M., Schmidt, M., VanBommel, S.J., 2017. APXS-derived chemistry of the Bagnold dune sands: comparisons with Gale Crater soils and the global Martian average. J. Geophys. Res. Planets 122. http://dx.doi.org/10.1002/2017JE005268.

Parsons, D.R., Wiggs, G.F.S., Walker, I.J., Ferguson, R.I., Garvey, B.G., 2004a. Numerical modeling of airflow over an idealized transverse dune. Environ. Modell. Software 19, 153–162.

Parsons, D.R., Walker, I.J., Wiggs, G.F.S., 2004b. Numerical modeling of flow structures over idealized transverse aeolian dunes of varying geometry. Geomorphology 59, 149–164.

Pelletier, J.D., Sherman, D.J., Ellis, J.T., Farrell, E.J., Jackson, N.L., Li, B., Nordstrom, K.F., Maia, L.P., Omidyeganeh, M., 2015. Dynamics of sediment storage and release on aeolian dune slip faces: a field study in Jericoacoara, Brazil. J. Geophys. Res. 120, 1911–1934. http://dx.doi.org/10.1002/2015JF003636.

Pla-Garcia, J., Rafkin, S.C.R., Kahre, M., Gomez-Elvira, J., Hamilton, V.E., Navarro, S., Torres, J., Marin, M., Vasavada, A.R., 2016. The meteorology of Gale crater as determined from rover environmental monitoring station observations and numerical modeling. Part I: Comparison of model simulations with observations. Icarus 280, 103–113.

Pye, K., Tsoar, H., 1990. Aeolian Sand and Sand Dunes. Unwin Hyman, London, pp. 396.

Runyon, K.D., Bridges, N.T., Ayoub, F., Newman, C.E., Quade, J.J., 2017. An integrated model for dune morphology and sand fluxes on Mars. Earth Planet. Sci. Lett. 257, 204–212.

Schatz, V., Tsoar, H., Edgett, K.S., Parteli, E.J.R., Herrmann, H., 2006. Evidence for indurated sand dunes in the Martian north polar region. J. Geophys. Res. (Planets) 111 (E4). http://dx.doi.org/10.1029/2005JE002514.

Shettigara, V.K., Sumerling, G.M., 1998. Height determination of extended objects using shadows in SPOT images. Photogramm. Eng. Remote Sens. 64 (1), 35–44.

Silvestro, S., Fenton, L.K., Vaz, D.A., Bridges, N.T., Ori, G., 2010. Ripple migration and dune activity on Mars: evidence for dynamic wind processes. Geophys. Res. Lett. 37.

Silvestro, S., Vaz, D.A., Fenton, L.K., Geissler, P.E., 2011. Active aeolian processes on Mars: a regional study in Arabia and Meridiani Terrae. Geophys. Res. Lett. 38.

Silvestro, S., Vaz, D.A., Ewing, R.C., Rossie, A.P., Fenton, L.K., Michaels, T.I., Flahaut, J., Geissler, P.E., 2013. Pervasive aeolian activity along rover Curiosity's traverse in Gale Crater, Mars. Geology 41, 483–486.

Smith, A.B., Jackson, D.W.T., Cooper, J.A.G., 2017. Three-dimensional airflow and sediment transport patterns over barchan dunes. Geomorphology 278, 28–42.

Sullivan, R., Greeley, R., Kraft, M., Wilson, G., Golombek, M., Herkenhoff, K., Murphy, J., Smith, P., 2000. Results of the imager for Mars pathfinder windsock experiment. J. Geophys. Res. Planets 105 (E10), 24547–24562.

Sullivan, R., Kok, J.F., 2017. Aeolian saltation on Mars at low wind speeds. J. Geophys. Res. Planets 122, 2111–2143.

Sutton, S.L.F., 2012. Avalanching on Aeolian Sand Dunes: Initiation, Sediment Redistribution and Classification. Ph.D. thesis. Trent University.

Sutton, S.L.F., McKenna Neuman, C., Nickling, W., 2013a. Avalanche grainflow on a simulated aeolian dune. J. Geophys. Res. Earth Surf. http://dx.doi.org/10.1002/jgrf.20130.

Sutton, S.L.F., McKenna Neuman, C., Nickling, W., 2013b. Lee slope sediment processes leading to avalanche initiation on an aeolian dune. JGR Earth Surf. http://dx.doi.org/10.1002/jgrf.20131.

Sweet, M.L., Kocurek, G., 1990. An empirical model of aeolian dune lee-face airflow. Sedimentology 37, 1023–1038.

Tischler, M.M., Bursik, I., Pitman, E.B., 2001. Kinematics of sand avalanches using particle-image velocimetry. J. Sed. Res. 71 (3), 355–364.

Vermeesch, P., Drake, N., 2008. Remotely sensed dune celerity and sand flux measurements of the world's fastest barchans (Bodele, Chad). Geophys. Res. Lett. 35. http://dx.doi.org/10.1029/2008GL035921.

Walker, I.J., 1999. Secondary airflow and sediment transport in the lee of a reversing dune. Earth Surf. Process. Landforms 24, 437–448.

Walker, I., Nickling, W., 2002. Dynamics of secondary airflow and sediment transport over and in the lee of transverse dunes. Progr. Phys. Geogr. 26 (1), 47–75. http://dx.doi.org/10.1191/0309133302pp325ra.

Wiggs, G.F.S., 2001. Desert dune processes and dynamics. Progr. Phys. Geogr. 25, 53–79.

Zurek, R.W., Barnes, J.R., Haberle, R.M., Pollack, J.B., Tillman, J.E., Leovy, C.B., et al., 1992. Mars. In: Kieffer, H.H. (Ed.), Univ. Arizona Press, Tucson, pp. 835–933.